

Vacancy-related defects and the E'_δ center in amorphous silicon dioxide: Density functional calculations

Blair R. Tuttle^{1,3} and Sokrates T. Pantelides^{1,2}¹*Department of Physics and Astronomy, Vanderbilt University, Nashville, Tennessee 37235, USA*²*Oak Ridge National Laboratory, Oak Ridge, Tennessee 37831, USA*³*Department of Physics, Penn State Behrend, Erie, Pennsylvania 16563, USA*

(Received 27 May 2008; revised manuscript received 28 January 2009; published 16 March 2009)

The microscopic identification of vacancy-related defects in silicon dioxide has been a major challenge. Particularly in amorphous silica, the role of vacancy clusters is still controversial. Experimental data have led to suggestions that the E'_δ center is a four-vacancy cluster instead of a single vacancy. Here we report density functional calculations that explore the energetics and electronic structure of single vacancies and clusters of four vacancies in realistic models of amorphous silica. A total of 76 O vacancies and 38 four-vacancy clusters were examined, and their energy levels and hyperfine parameters were calculated. Results for single vacancies compare well to previous theory. A key result for four-vacancy clusters is that relaxations localize the unpaired electron preferentially on one Si atom, resulting in a strongly anisotropic electron-paramagnetic-resonance signal. Electrons at single vacancies have a more benign anisotropy which is more compatible with the observed isotropic signal.

DOI: 10.1103/PhysRevB.79.115206

PACS number(s): 61.72.J–

I. INTRODUCTION

Oxygen vacancies are the most common defects found in silicon dioxide. Several vacancy-related defects (VRDs) have been classified as E' centers based on their signatures observed with electron paramagnetic resonance (EPR).^{1–3} Determining the microscopic structure of VRDs from EPR signatures has been a challenge for many decades.^{1–8} Most VRDs originally observed by EPR in quartz^{3,5} also have analogous centers in amorphous silicon dioxide (a -SiO₂).^{1,2,5} The latter material has garnered broad interest because a -SiO₂ is a ubiquitous component of electronic and optical devices. Moreover, VRDs are a persistent cause of device degradation^{9–11} even in transistors with alternative high- K gate dielectrics.^{12,13}

In quartz, the primary VRD, called the E'_1 center, was first observed over 40 years ago³ but its identification became definitive only after many years of study because of a rather unexpected behavior, unveiled by theory.⁷ Although in the neutral state the two neighboring Si atoms rebond and form a Si-Si bond, in the EPR-active positively charged state, one of the Si atoms puckers backward and bonds to a backside oxygen, leaving a dangling bond on the other Si atom.⁷

In a -SiO₂, the two common VRDs are the E'_γ and E'_δ centers. These two VRDs have been well characterized in bulk a -SiO₂ (Refs. 2 and 6) and similar defects have been observed in modern transistors.^{11,13} The E'_γ center has an anisotropic spin distribution characteristic of a dangling bond and is understood as a puckered vacancy, analogous to the E'_1 center observed in quartz.^{5–7} Discovered in the 1980s, the E'_δ center has a nearly isotropic-spin distribution and a hyperfine (HF) splitting of only ~ 10 mT compared with the ~ 40 mT for the E'_γ center. No analogous center has been observed in quartz.⁶ Definite identification of E'_δ has remained elusive. The nearly isotropic EPR signal and the fact that the HF splitting is $\frac{1}{4}$ that of E'_γ led to the suggestion that the E'_δ center corresponds to a larger vacancy cluster with four

E'_γ -like dangling bonds.^{1,2,6} An alternative model, simply a single oxygen vacancy that remains a Si-Si dimer even in the positive state, has been supported by calculations of the HF splitting^{14–16} and by the finding that, in a -SiO₂, $\sim 80\%$ of O vacancies do indeed remain in the dimer configuration when positively charged.⁴ Recently, Buscarino *et al.*^{1,2} presented experimental data that appear to rule out the dimer model but are consistent with a cluster of four oxygen vacancies. However, Refs. 1 and 2 do not offer an explanation for the lack of a signal due to single vacancies. A comprehensive model for VRDs and the E'_δ center in amorphous silicon dioxide remains elusive.

We present first-principles electronic-structure calculations of VRDs in SiO₂ including single oxygen vacancies and clusters of vacancies. In all cases, we investigated the positively charged states of configurations in which no E'_γ -like puckering occurs (“dimer vacancies”). The most important result is the ²⁹Si isotropic hyperfine values for dozens of VRDs. In addition, we present the structure, dynamics, and electronic structure of vacancy clusters. Based on these results, we find that, compared to the vacancy clusters, the single vacancy is more consistent with the experimental characteristics of the E'_δ center. The rest of this paper is organized as follows: in Sec. II, we present our methodology; in Sec. III, we report our results; in Sec. IV, we analyze the results to determine the relative formation energies for vacancy clusters; and in Sec. V, we compare our results to experiments and present our conclusions.

II. METHODOLOGY

The amorphous silica model used in this study was generated with an empirical-potential Monte Carlo bond switching method.^{17–19} The model includes 38 SiO₂ units enclosed within a cubic supercell with sides 11.9 Å long. The bonding is consistent with experiments. There are no coordination

TABLE I. The isotropic ^{29}Si hyperfine parameter (for the Si atom in bold) is reported for several molecules. The present CP-PAW method compares favorably to experiment (Ref. 23).

Molecule	Isotropic ^{29}Si HF parameter (mT)	
	Present	Experiment
Si (CH ₃) ₃	15.8	18.1
Si [Si(CH ₃) ₃] ₃	5.8	6.4
Si[Si (CH ₃) ₃] ₃	0.1, 0.3, 1.0	0.7
{C ₆ H ₅ [Si -(CH ₃) ₃]} ⁻¹	0.1	0.5
{C ₆ H ₂ O ₂ [Si -(CH ₃) ₃] ₂ } ⁻¹	0.1	0.2

defects and only rings of four or more Si atoms are found. The model has been employed previously to elucidate the nature of water in silica-based network glasses.¹⁹

Density functional calculations were performed to examine the properties of VRDs. Generalized-gradient corrected exchange-correlation functionals and one special k point at $\frac{1}{2}$ (111) were used for all calculations. To calculate energetics, defect levels, and reaction barriers, we used the VASP code.²⁰ Ultrasoft pseudopotentials, a plane-wave basis cutoff of 22 Ry, and a force tolerance of 0.05 eV/Å were employed. Furthermore, reaction barriers were calculated using the climbing elastic-band method.²¹ The CP-PAW program was used to further relax selected structures and to calculate HF parameters for various EPR-active vacancy defects.²² The projector augmented wave approach was employed using 30 Ry for the cutoff of the plane-wave basis. Comparing the CP-PAW and VASP calculations indicates that relative energies are numerically converged to less than 0.1 eV. However, treating charged defects within periodic systems leads to spurious charge and dipole interactions between periodic images. No *ad hoc* corrections have been applied to the reported energy barrier results. Since saddle-point configuration has more diffuse wave functions, we expect the corrected barriers to be slightly larger than those reported here. These considerations do not affect the main conclusions.

The experimentally observed HF splitting is determined by the isotropic ^{29}Si HF parameter (a_{iso}), which can be calculated using the equation $a_{\text{iso}} = 31.7 \text{ mT } \rho_{\text{spin}}(^{29}\text{Si})$, where $\rho_{\text{spin}}(^{29}\text{Si})$ is the spin density in atomic units at the nucleus of the silicon atom considered. As illustrated in Table I, the present CP-PAW implementation is capable of reproducing experimental results over the range of interest, i.e., from less than 1 to 20 mT.²³ The molecules were chosen for Table I based on having similar Si bonding and similar ^{29}Si HF values. Overall, the present results tend to be lower than experiment by 2 mT or less. The molecule Si[Si(CH₃)₃]₃ is particularly instructive. The main silicon defect is calculated to have a ^{29}Si isotropic HF value of 5.8 mT compared to the value of 6.4 mT from experiment. The three neighboring silicon atoms should have identical HF values by symmetry. In our method, symmetry was not imposed. Although the resulting structure is reasonably symmetric, we find variable HF values in the range of 0.1–1.0 mT compared to the single experimental result of 0.7 mT. Based on the above comparisons

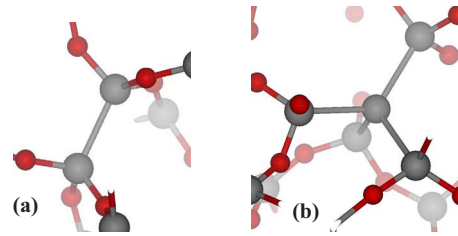


FIG. 1. (Color online) Example for the neutral state of (a) the oxygen vacancy dimer, called a Si₂ defect, and (b) four vacancies clustered around a central silicon atom, called a Si₅ defect. Large gray spheres are silicon atoms and small dark (red) spheres are oxygen atoms.

with experiment and the range of structures considered below, we estimate the present method's error bars are +1.0 and -0.5 mT for our reported HF values.

III. RESULTS

Models of isolated single oxygen vacancies were generated by removing one oxygen atom from our amorphous SiO₂ supercell. We examined all of the 76 oxygen vacancy sites. In all cases, the vacancies relaxed to form Si-Si dimer bonds (called Si₂ defects for short) in both the neutral and positive charge states. In the neutral charge state, the resulting Si-Si bonds have an average length of 2.46 Å with a range of lengths between 2.3 and 2.7 Å. A ball-and-stick model of a neutral Si₂ defect is shown in Fig. 1. In the neutral case, the formation energy was correlated with the final Si-Si bond length, with shorter bonds representing lower energy structures. There was a range of more than 1 eV between the lowest-energy and highest-energy configurations. With a reference of O₂ in vacuum, the average vacancy formation energy is +2.7 eV, with a spread of formation energies between 2 and 4 eV. Figure 2 shows a histogram of the number of defects versus formation energy using a 0.2 eV bin size. The electronic structure of the vacancy defects includes one filled defect level near the valence-band edge and one empty level below the conduction-band edge. The average +/0 acceptor level is $\sim E_V + 0.5 \text{ eV}$.

In the positive charge state, the Si-Si bond length ranges from 2.8 to 3.2 Å with an average bond length of 2.94 Å.

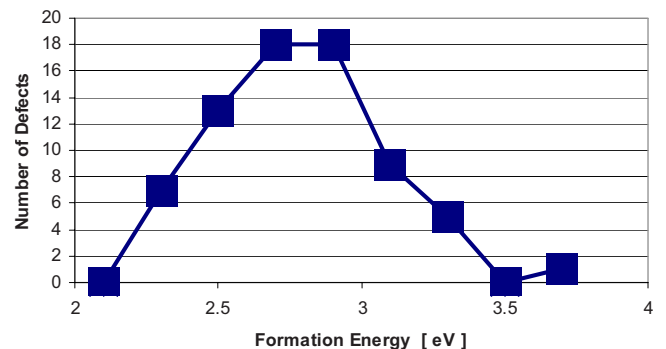


FIG. 2. (Color online) Histogram of formation energy for the single vacancy defects called Si₂ defects.

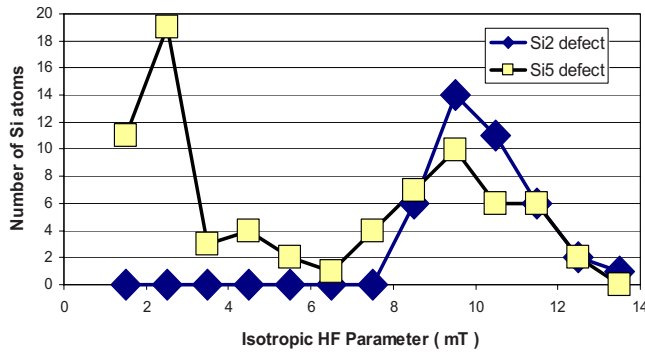


FIG. 3. (Color online) Histogram of the calculated HF parameters for both the Si_2 and the Si_5 defects. Both Si_2 and Si_5 defects have a broad peak centered at ~ 10 mT consistent with experimental observations. The bin size is 1 mT. Only atoms with HF parameters greater than 1 mT are included in the histogram.

The defect spin density mainly spreads between the two Si atoms of the dimer bond. The puckered configuration was not considered. The isotropic ^{29}Si HF parameters were calculated for all silicon atoms in 40 of the 76 Si_2 defect models. Atomic level analysis of the spin density indicates that only the two Si atoms associated with the Si_2 defects contribute to the histogram. All other silicon atoms had a ^{29}Si HF parameter less than 1 mT and would be invisible during EPR HF measurements. For the two silicon atoms of the vacancy, the isotropic ^{29}Si HF parameters are within the range of 8–12 mT. Figure 3 combines all the ^{29}Si HF parameter calculations for all atoms in all models into a single histogram. The results for Si_2 defects are presented as dark boxes in Fig. 3. The histogram of the Si_2 defect ^{29}Si HF parameters has a single peak ~ 10 mT, consistent with experiments and previous theoretical studies.^{14–16}

Cluster models including four vacancies (called Si_5 defects for short) were generated in our model amorphous silicon dioxide. After removing four oxygen atoms, each bound to a central silicon atom, four Si-Si bonds form, as illustrated in Fig. 1(b). All 38 distinct Si_5 defect models were considered. In the neutral charge state, the Si-Si bonds of the Si_5 defect have an average length of 2.63 Å, slightly larger than in the case of the Si_2 defect. The average formation energy is 2.6 eV with Fig. 4 showing the histogram of formation energies using a 0.2 eV bin size. It is noteworthy that the range

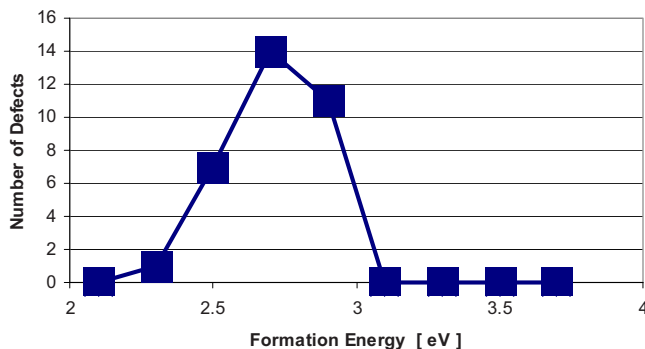


FIG. 4. (Color online) Histogram of formation energy for the four-vacancy cluster defects called Si_5 defects.

of formation energies is smaller for the Si_5 defects than for the Si_2 defects. Compared to the single vacancy, the electronic structure of the Si_5 defect is more complicated, with four occupied and unoccupied bands near the valence-band and conduction-band edges, respectively. For each Si_5 defect the occupied defect levels occur between 0 and 1.5 eV above the valence-band edge, with wide variations in the level positions between the various Si_5 defects. The average $+/0$ acceptor level is $\sim E_V + 1.0$ eV.

In the positive charge state of the Si_5 defect, one of the four Si-Si bonds elongates substantially with a Si-Si distance greater than 3.5 Å whereas the other three Si-Si bonds are typically around 2.6 Å. The isotropic ^{29}Si HF parameters were calculated for all silicon atoms in all the models. The results are presented in Fig. 3 as light boxes. The histogram for the Si_5 defect has two peaks: one broad peak centered ~ 10 mT and another sharper peak at ~ 2 –3 mT. Analysis of the atom specific data finds that the spin density associated with the ~ 10 mT peak is due to the single outer silicon of the elongated bond. The peak at ~ 2 –3 mT is due to the central silicon and sometimes to another silicon atom within the cluster. Silicon atoms outside of the Si_5 cluster have negligible (< 1 mT) ^{29}Si isotropic HF parameters. In both the E'_γ defect and in the Si_5 defect, the spin density mainly localizes on a single Si atom. The difference between the two is that the Si_5 defect's spin density is extended over a broader region between an elongated bond whereas, for the E'_γ defect, the spin density localizes around the single silicon dangling bond. The broader spin-density distribution for the Si_5 defect results in a lower spin density at the silicon atom of the defect and explains the much lower isotropic ^{29}Si HF value.

For the Si_5 defect in the positive charge state, one of the four Si-Si bonds elongates significantly more than the other three. However, the defect does not strongly favor one Si-Si bond to be longer than the others. In Fig. 5, we show a positively charged Si_5 defect in two of the four distinct configurations. The elongated bond, denoted in Fig. 5 by the thin dark line, is ~ 3.6 Å in the cases shown. Again, the defect's spin density is mainly distributed in the region of the elongated bond. The spin density is localized directly on the outer Si atom resulting in a ^{29}Si HF parameter between 7 and 11 mT, i.e., within the range reported in Fig. 3. Only ~ 0.2 eV separates the highest from the lowest energy configurations. In addition, the barrier for the cluster to change from one long Si-Si bond to another is found to be about 0.6 eV.

While here we focus on four-vacancy clusters (Si_5 defects), other vacancy clusters can form. To provide an illustrative view of such clusters, we construct several models for three-vacancy and five-vacancy clusters by choosing a single low energy Si_5 defect, then adding or subtracting an oxygen atom. In these vacancy cluster models, we find that the defect spin density is also localized on a single outer silicon atom, as in the case of the Si_5 defect. We find that the average main ^{29}Si HF parameter for the three-vacancy and five-vacancy clusters are ~ 8 and ~ 13 mT, respectively. These average values are distinct from the average of the Si_5 defect cluster but the results are within the range of values reported in Fig. 3.

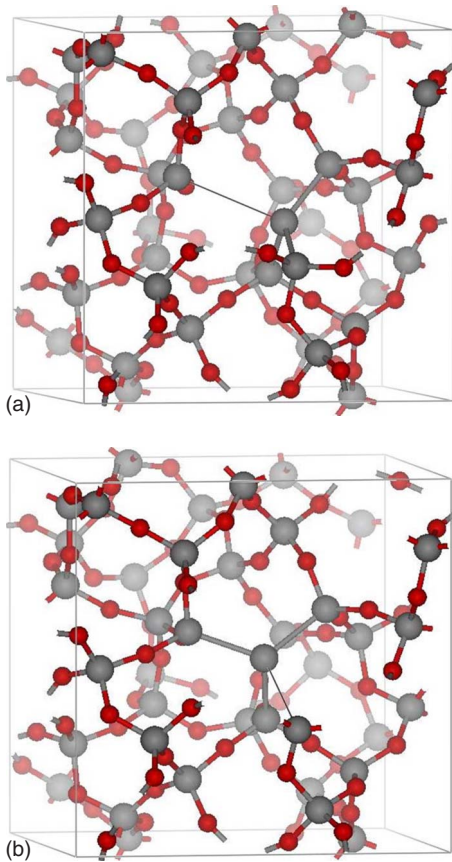


FIG. 5. (Color online) Two configurations of a single Si_5 defect are shown for the EPR-active positive charge state. Each configuration involves a different elongated Si-Si bond denoted by the thin dark line. These configurations are close in energy with the barriers between them being approximately 0.6 eV.

IV. ANALYSIS

For vacancy clusters to exist in large concentrations, the conversion of single vacancies into clusters must be exothermic. In the present calculations, we find that on average the conversion of four Si_2 defects into a Si_5 defect is indeed exothermic by 0.07 eV per Si-Si bond. The Si_5 defects investigated here experience significant strain since the supercell's volume is not allowed to relax. If the oxide fully relaxes, then the energy differences between clusters is simply the varying cost of energy due to the varying oxidation states of the silicon atoms involved. Using bond-energy empirical potentials as in Refs. 17, 24, and 25, one can associate an energy to a particular atom in a system. Recent comparisons between bond-energy empirical potentials and *ab initio* calculations have shown that, when bond strain is removed, the energetics of a system of Si-O and Si-Si bonds can be written in terms of just the energetics of the respective oxidation states of the silicon atoms involved.^{24,25} Using the results of Refs. 24 and 25, we can compare the energetics of idealized oxygen vacancy clusters, with no bond strain, by comparing the oxidation state energies of the silicon atoms in the cluster. Compared to fully oxidized (Si^{+4}) or fully unoxidized (Si^0) silicon atoms, partially oxidized atoms are higher in energy. Specifically, Si^{+1} , Si^{+2} , and Si^{+3} atoms are on average

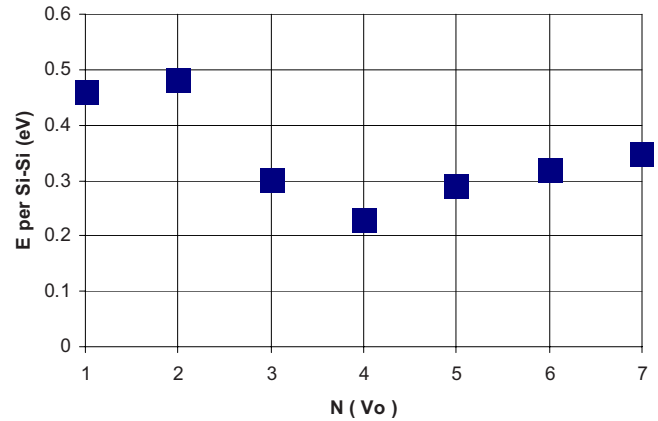


FIG. 6. (Color online) Energetics of vacancy clusters: the energy per Si-Si bond is plotted versus $N(V_o)$, the number of oxygen vacancies in a cluster. The Si_5 defect is a cluster with $N(V_o)=4$. The zero of energy refers to a Si-Si bond in bulk crystalline silicon. The plot shows that Si_5 defects are energetically the most favorable vacancy clusters but these are still higher in energy than Si-Si bonds in silicon.

0.49, 0.51, and 0.23 eV higher in energy, respectively. Using these average numbers, we calculate the energy per Si-Si bond for clusters of various sizes with the results reported in Fig. 6. The energy of a Si-Si bond in bulk crystalline silicon is chosen as the zero of energy. Clusters of three vacancies or more are favored over isolated single vacancies, i.e., Si_2 defects. The Si_5 defect is a cluster of four vacancies and is the most stable, which is 0.23 eV per Si-Si more favorable than the Si_2 defect. The special stability of the Si_5 occurs because the central atom is in a favorable unoxidized state. While formation energy considerations clearly favor some vacancy clustering, oxide growth conditions are important for determining relative concentrations of VRDs, and the growth of clusters may be limited by entropic and kinetic effects. Specifically, in thermal oxides grown on silicon, cluster formation is suppressed since vacancies in the oxide can favorably recombine with bulk silicon at the growth interface.

V. DISCUSSION

While the presence of single vacancies in $a\text{-SiO}_2$ is well known based on the EPR signatures of E'_γ centers, the presence of vacancy clusters has not been established. Recently, Buscarino *et al.*^{1,2} analyzed their data following the procedure of Zhang and Leisure,²⁶ who found that four silicon atoms are involved in the E'_δ center. To determine the number of HF active silicon atoms in the E'_δ center, they calculate the ratio of the HF doublet EPR intensity to the main resonance EPR intensity. This analysis uses the E'_β or the E'_γ center for the purpose of calibration. The implicit assumption is that the silicon atoms participating in the E'_δ center have the same kind of Si dangling bonds as either the E'_β or the E'_γ centers. However, due to Jahn-Teller distortions, defect clusters of silicon dangling bonds reconstruct to form new bonds. This reconstruction is not unexpected as Si dangling bonds at a vacancy in crystalline Si have long been known to undergo such rebonding.^{27,28} As discussed in Refs. 4, 14, and 16, the

positively charged vacancy in SiO_2 , when dimerized in the way usually attributed to a E'_δ center, involves two Si sp^3 orbitals that form a bonding orbital occupied by a single electron, not two isolated Si sp^3 orbitals. Reconstructions are more dramatic for the Si_5 defect where the hole disrupts one of the four Si-Si bonds, leaving the other three virtually intact. For both the Si_2 and Si_5 defects the assumption of the experimental data analysis in Ref. 1 fails to be verified by theoretical calculations. Therefore, the available experimental data do not constrain the number of silicon atoms involved in the E'_δ center.

The histogram of HF results presented in Fig. 4 indicates that, compared to the vacancy cluster (Si_5 defect), the single vacancy (Si_2 defect) model is more consistent with the experimental HF results for the E'_δ center. The distribution of the single vacancy HF values peak around 10 mT with no other peaks. In contrast, the Si_5 defects result in a broad distribution centered around 10 mT with an extra peak at 2–3 mT. This lower peak provides a definitive test for clusters and no lower peak has been reported to date. From the comparisons of our results and experiments, the single vacancy (Si_2 defect) is a much stronger candidate for the E'_δ center.

Regarding the identification of the E'_δ center with the single vacancy, one remaining concern is the observed isotropy of the E'_δ center g tensor. While calculations of g tensors are beyond the scope of the present work, based on our electronic-structure calculations, we can offer some insight.

The Si_5 defects are found to localize on a single silicon atom and should have a more anisotropic g tensor than the Si_2 defects. However, at room temperature, the positively charged Si_5 defects will dynamically resonate between the four configurations since the barrier for hopping is low (~ 0.6 eV). The overall effect is a more isotropic g value. However, this dynamic isotropy would be frozen out at low temperatures. In fact, the experiments of Refs. 6 and 9 performed at 77 and 4 K, respectively, do not result in any remarkable change in the isotropy of the E'_δ center, suggesting that vacancy clusters are not responsible for the E'_δ center.

In summary, the properties of VRDs in silicon dioxide have been calculated with state-of-the-art first-principles methods. The properties of vacancy clusters are presented and shown to be inconsistent with prevailing observations of the E'_δ center. However, single isolated vacancies are shown to provide a compelling model for the E'_δ center. Overall, this work elucidates the nature of VRDs in amorphous silicon dioxide.

ACKNOWLEDGMENTS

This work was supported in part by the Air Force Office of Scientific Research under a MURI grant (Grant No. FA9550-05-1-06) and by the U.S. Navy. Calculations were performed on the NCSA supercomputers in Urbana, IL.

-
- ¹G. Buscarino, S. Agnello, and F. M. Gelardi, Phys. Rev. Lett. **94**, 125501 (2005).
²G. Buscarino, S. Agnello, and F. M. Gelardi, Phys. Rev. B **73**, 045208 (2006).
³R. A. Weeks and C. M. Nelson, J. Am. Ceram. Soc. **43**, 399 (1960).
⁴Z. Y. Lu, C. J. Nicklaw, D. M. Fleetwood, R. D. Schrimpf, and S. T. Pantelides, Phys. Rev. Lett. **89**, 285505 (2002).
⁵M. Boero, A. Pasquarello, J. Sarnthein, and R. Car, Phys. Rev. Lett. **78**, 887 (1997).
⁶D. L. Griscom and E. J. Friebele, Phys. Rev. B **34**, 7524 (1986).
⁷K. L. Yip and W. B. Fowler, Phys. Rev. B **11**, 2327 (1975).
⁸S. T. Pantelides, Z.-Y. Lu, C. Nicklaw, T. Bakos, S. N. Rashkeev, D. M. Fleetwood, and R. D. Schrimpf, J. Non-Cryst. Solids **354**, 217 (2008).
⁹K. Vanheusden and A. Stesmans, J. Appl. Phys. **74**, 275 (1993).
¹⁰W. L. Warren, D. M. Fleetwood, M. R. Shaneyfelt, J. R. Schwank, P. S. Winokur, and R. A. B. Devine, Appl. Phys. Lett. **62**, 3330 (1993).
¹¹W. L. Warren, M. R. Shaneyfelt, D. M. Fleetwood, J. R. Schwank, P. S. Winokur, and R. A. B. Devine, IEEE Trans. Nucl. Sci. **41**, 1817 (1994).
¹²C. J. Forst, C. R. Ashman, K. Schwarz, and P. E. Blochl, Nature (London) **427**, 53 (2004).
¹³J. T. Ryan, P. M. Lenahan, G. Bersuker, and P. Lysaght, Appl. Phys. Lett. **90**, 173513 (2007).
¹⁴P. E. Blochl, Phys. Rev. B **62**, 6158 (2000).
¹⁵A. S. Mysovsky, P. V. Sushko, S. Mukhopadhyay, A. H. Edwards, and A. L. Shluger, Phys. Rev. B **69**, 085202 (2004).
¹⁶J. R. Chavez, S. P. Karna, K. Vanheusden, C. P. Brothers, R. D. Pugh, B. K. Singaraju, W. L. Warren, and R. A. B. Devine, IEEE Trans. Nucl. Sci. **44**, 1799 (1997).
¹⁷Y. Tu and J. Tersoff, Phys. Rev. Lett. **84**, 4393 (2000).
¹⁸K. O. Ng and D. Vanderbilt, Phys. Rev. B **59**, 10132 (1999).
¹⁹I. G. Batyrev, B. R. Tuttle, D. M. Fleetwood, R. D. Schrimpf, L. Tsetseris, and S. T. Pantelides, Phys. Rev. Lett. **100**, 105503 (2008).
²⁰G. Kresse and J. Hafner, J. Phys.: Condens. Matter **6**, 8248 (1994).
²¹G. Henkelman, B. P. Uberuaga, and H. Jónsson, J. Chem. Phys. **113**, 9901 (2000).
²²P. E. Blochl, Phys. Rev. B **50**, 17953 (1994).
²³L. Hermosilla, P. Calle, J. M. García de la Vega, and C. Sieiro, J. Phys. Chem. A **109**, 7626 (2005).
²⁴A. Bongiorno and A. Pasquarello, Phys. Rev. B **62**, R16326 (2000).
²⁵D. R. Hamann, Phys. Rev. B **61**, 9899 (2000).
²⁶L. Zhang and R. J. Leisure, J. Appl. Phys. **80**, 3744 (1996).
²⁷G. A. Baraff, E. O. Kane, and M. Schluter, Phys. Rev. Lett. **43**, 956 (1979).
²⁸N. O. Lipari, J. Bernholc, and S. T. Pantelides, Phys. Rev. Lett. **43**, 1354 (1979).